ISSN 1674-1056
http://cpb.iphy.ac.cn
http://iopscience.iop.org/cpb
中国物理 B
Chinese Physics
中国物理
Chinese Physics B

Aging mechanism of GaN-based yellow LEDs with V-pits

Tian-Ran Zhang(张天然), Fang Fang(方芳), Xiao-Lan Wang(王小兰), Jian-Li Zhang(张建立), Xiao-Ming Wu(吴小明), Shuan Pan(潘栓), Jun-Lin Liu(刘军林), Feng-Yi Jiang(江风益)

Citation: Chin. Phys. B . 2019, 28(6): 067305. **doi:** 10.1088/1674-1056/28/6/067305
Journal homepage: http://cpb.iphy.ac.cn; http://iopscience.iop.org/cpb

What follows is a list of articles you may be interested in

Low specific on-resistance GaN-based vertical heterostructure field effect transistors with nonuniform doping superjunctions

Wei Mao(毛维), Hai-Yong Wang(王海永), Peng-Hao Shi(石朋毫), Xiao-Fei Wang(王晓飞), Ming Du(杜鸣), Xue-Feng Zheng(郑雪峰), Chong Wang(王冲), Xiao-Hua Ma(马晓华), Jin-Cheng Zhang(张进成), Yue Hao(郝跃)
Chin. Phys. B . 2018, 27(4): 047305. **doi:** 10.1088/1674-1056/27/4/047305

Improved performance of AlGaN/GaN HEMT by N_2O plasma pre-treatment

Mi Min-Han, Zhang Kai, Zhao Sheng-Lei, Wang Chong, Zhang Jin-Cheng, Ma Xiao-Hua, Hao Yue
Chin. Phys. B . 2015, 24(2): 027303. **doi:** 10.1088/1674-1056/24/2/027303

A two-dimensional fully analytical model with polarization effect for off-state channel potential and electric field distributions of GaN-based field-plated high electron mobility transistor

Mao Wei, She Wei-Bo, Yang Cui, Zhang Chao, Zhang Jin-Cheng, Ma Xiao-Hua, Zhang Jin-Feng, Liu Hong-Xia, Yang Lin-An, Zhang Kai, Zhao Sheng-Lei, Chen Yong-He, Zheng Xue-Feng, Hao Yue
Chin. Phys. B . 2014, 23(8): 087305. **doi:** 10.1088/1674-1056/23/8/087305

Non-recessed-gate quasi-E-mode double heterojunction AlGaN/GaN high electron mobility transistor with high breakdown voltage

Mi Min-Han, Zhang Kai, Chen Xing, Zhao Sheng-Lei, Wang Chong, Zhang Jin-Cheng, Ma Xiao-Hua, Hao Yue
Chin. Phys. B . 2014, 23(7): 077304. **doi:** 10.1088/1674-1056/23/7/077304

Kink effect in current–voltage characteristics of a GaN-based high electron mobility transistor with an AlGaN back barrier

Ma Xiao-Hua, Lü Min, Pang Lei, Jiang Yuan-Qi, Yang Jing-Zhi, Chen Wei-Wei, Liu Xin-Yu
Chin. Phys. B . 2014, 23(2): 027302. **doi:** 10.1088/1674-1056/23/2/027302

Aging mechanism of GaN-based yellow LEDs with V-pits*

Tian-Ran Zhang(张天然), Fang Fang(方芳)†, Xiao-Lan Wang(王小兰), Jian-Li Zhang(张建立), Xiao-Ming Wu(吴小明), Shuan Pan(潘栓), Jun-Lin Liu(刘军林), and Feng-Yi Jiang(江风益)

National Institute of LED on Silicon Substrate, Nanchang University, Nanchang 330096, *China*

(Received 13 March 2019; revised manuscript received 2 April 2019; published online 8 May 2019)

GaN-based yellow light-emitting diodes (LEDs) on Si substrates are aged at a direct current density of 50 A/cm^2 for 500 h. After the aging process, it can be found that the LEDs have a stable electrical property but their light output power is decayed by 4.01% at 35 A/cm^2. Additionally, the aging mechanism of GaN-based yellow LED is analyzed. It is found that the decay of light output power may be attributed to the following two reasons: one is the increase of Shockley–Rrad–Hall recombination and the other is the change of the transport path of holes via V-pits after aging, which may induce the radiative recombination current to decrease. In this paper, not only the aging mechanism of GaN-based yellow LED is investigated, but also a new possible research direction in LED aging is given.

Keywords: GaN-based, yellow LED, aging mechanisms, V-pits

PACS: 73.61.Ey, 78.60.Fi, 73.21.Fg, 73.21.Cd **DOI:** 10.1088/1674-1056/28/6/067305

1. Introduction

Over the past few years, GaN-based light-emitting diodes (LEDs) have shown excellent performance and have been applied to solid state lighting (SSL) systems. The color-mixed approach, that is, component red, green, yellow and blue LED are mixed, is an ideal way to generate white light for SSL.[1] However, considering the difficult growth and low efficiency of the yellow InGaN-based LED, yellow GaN-based LED is a weak point of color-mixed SSL, which is mainly attributed to high indium content. In order to gain a high efficiency yellow GaN-based LED, great efforts have been made and have made great advances.[2,3]

Nevertheless, with the enhanced performance of yellow GaN-based LED, the reliability of the yellow LED is also the limitation for color-mixed SSL. For reliability studies, the accelerated aging test is the main research method. The aging mechanism of GaN-based blue LED has been investigated, and mainly related to the generation of defects within an active region of the device,[4–6] interdiffusion on metal-semiconductor interface,[7,8] serious deterioration of the package,[9] and electromigration between the metal electrode and semiconductor,[10] *etc*.

Additionally, it was found that V-shape pits (V-pits) exist in GaN-based LED, which can screen dislocation, and improve the radiative recombination.[11] Besides, V-pits can also make contribution to the reducing reverse leakage current.[12] For hole injection, it was also found that the V-pits give a path for hole injection through sidewall of V-pits and assist holes in being transferred near the n-side of device, realizing more hole distributions over multiple quantum wells (MQWs).[13,14]

However, the aging mechanisms of yellow GaN-based LEDs was barely investigated. Furthermore, considering that V-pits make much contribution to the LED performance whether the V-pits have an effect on the aging process is unknown, it is necessary to investigate the aging mechanism of yellow GaN-based LED and the effect of V-pits on the aging process.

2. Experiments

The samples in this study were grown on patterned Si (111) substrates by metal organic chemical vapor deposition (MOCVD). As shown in Fig. 1, the epitaxial structure of the sample was started with an AlN buffer layer, and then a 3.3-μm Si-doped n-GaN layer was grown on it. Subsequently, 32-period 5-nm InGaN/2-nm GaN superlattice layers (SLs) were deposited on n-GaN layer. After that, 10-nm Si-doped low temperature-GaN was grown before 8-period InGaN/GaN MQW. The p-type layers consisted of p-AlGaN electron barrier layer (EBL), hole injection layer, and heavily doped p-GaN contact layer. After the growth process, the epitaxial wafers were fabricated into vertical LEDs with the size of 1 mm×1 mm. After the chip process, ten LED chips were selected and packaged in an LUXEON structure, whose dominant wavelength (DW) is 561 nm at 35 A/cm^2. A high direct current (DC) of 500 mA (50 A/cm^2) was applied to each tube at 40 °C ambient temperature, thus it was subjected to an electrically stress and lasted 500 h (*i.e.*, the tube was aged for 500 h). While in the aging process, the light output power (LOP) and current–voltage (*I*–*V*) curves of samples were measured at regular intervals by CAS140CT spectrograph and

*Project supported by the National Natural Science Foundation for Young Scientists of China (Grant Nos. 61704069 and 51602141) and the National Key Research and Development Program of China (Grant No. 2016YFB0400601).

†Corresponding author. E-mail: 41770109@qq.com

© 2019 Chinese Physical Society and IOP Publishing Ltd

ISP250-211 integrating sphere. In order to clarify the associated failure mechanisms, the temperature-dependent electroluminescence (TDEL) measurements of the device were performed before and after the aging process.

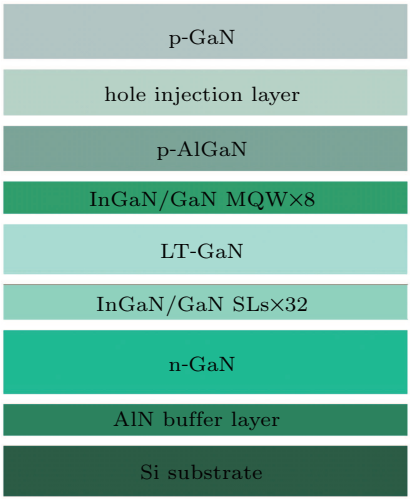


Fig. 1. Schematic epitaxial structure of samples in aging test.

3. Results and discussion

The average of normalized LOPs for ten aged chips tested at 35 A/cm^2 in 500-h aging process is shown in Fig. 2(a). It can be seen that after the aging process, the LOP decreases by 4.01%. The inset in Fig. 2(a) displays the normalized *L*–*I* curves for sample before and after aging. One can find that the LOP decreases slightly. In this paper, the decrease of the LOP is mainly attributed to the increase of Shockley–Rrad–Hall (SRH) recombination and the reduction of the radiative recombination current, which will be discussed below.

For the InGaN-based LED, the carrier recombination mechanism can be inferred by *S* value according to $L \propto I^S$. When the SRH recombination dominates, *S* equals 2. While the radiative recombination dominates, *S* value is 1. And *S* value less than 1 means carrier leakage by overflowing quantum wells (QWs).[15] Figure 2(b) shows the *S* values calculated by *L*–*I* curves before and after the aging process. With the aging time increasing, the *S* value rises at each test current density. Figure 2(b) can be divided into the upper and lower region by the $S = 1$ line. For the upper region, *S* value is greater than 1 and shifts from 1.23 to 1.30 at 0.35 A/cm^2, which is closer to 2. This phenomenon indicates that the non-radiative recombination increases, which is attributed to the increase of SRH recombination. For the lower region, *S* value is less than 1, which is mainly due to the carrier overflowing QWs. Similarly, at the current density of 10 A/cm^2, *S* value increases from 0.83 to 0.89 after aging and gets closer to 1. This indicates that the number of overflowing carriers decreases, which is also attributed to the increase of the SRH recombination and consumes more carriers.

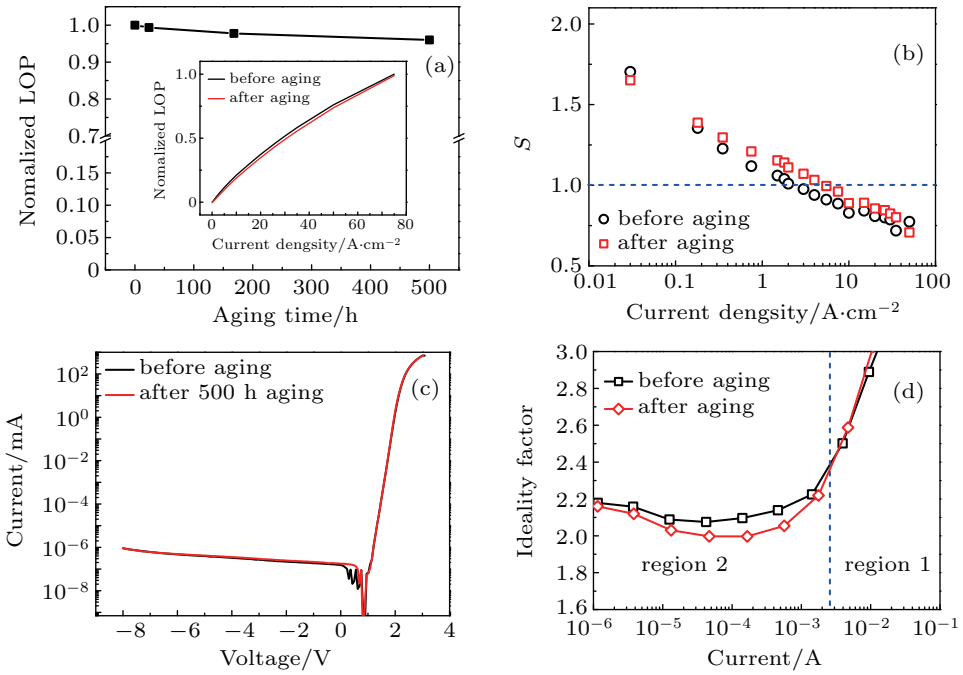


Fig. 2. (a) Average LOP of analyzed sample tested at 35 A/cm^2 in 500-h aging process. Inset shows *L*–*I* curves for sample before and after aging. (b) *S* value *versus* current density before and after aging process. (c) The *I*–*V* characteristic of sample before and after aging. (d) Ideality factors *versus* current density for the sample before and after aging.

The current–voltage (*I*–*V*) curves for the sample before and after a 500 h aging process are plotted in Fig. 2(c), and there is no significant increase in leakage current after aging, which means that the samples have stable electrical property. It is known that the ideality factor (*n*) can be used to analyze the recombination mechanism of the diode. An ideality factor close to 1 means that the direct band-to-band recombination is dominated. A value close to 2 is attributed to the SRH recom-

bination via defect level. And the high ideality factor ($n \gg 2$) means defect-assisted tunneling phenomenon.[16–18] Consequently, the ideality factors for samples are calculated according to I–V curves and the results are shown in Fig. 2(d) which can be divided into two regions. In region 1, one can find that the ideality factor increases rapidly with the current density increasing, which is attributed to the series resistance.[18] In region 2, both the ideality factor for sample before and after aging are both greater than 2. However, the ideality factor after the aging process is getting closer to 2, which indicates that the recombination mechanism changes after aging. Before aging, the defect-assisted tunneling dominates. While after aging, the SRH recombination via defect dominates instead. That is to say, more SRH recombination centers are generated after aging, which is consistent with the conclusion obtained by the change of the S value.

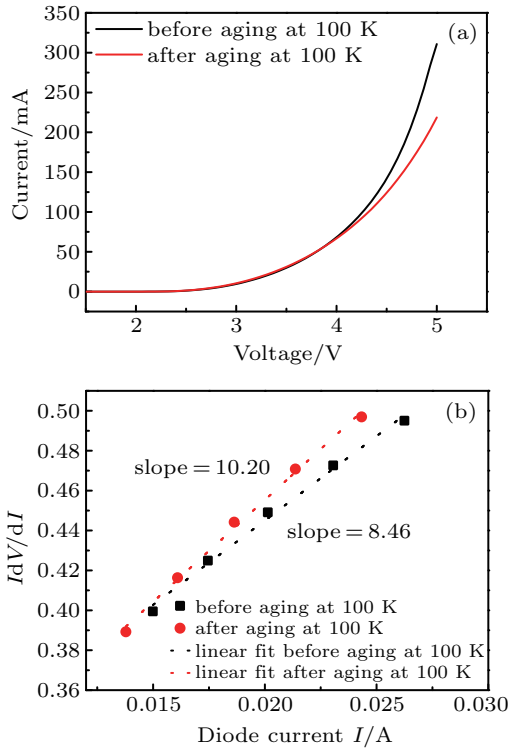


Fig. 3. (a) The I–V curve of sample before and after 500-h aging at 100 K. (b) Calculated series resistance via slope of a $(I\mathrm{d}V/\mathrm{d}I)$–$I$ for sample at 100 K before and after aging.

Then, the photoelectric properties of the sample before and after aging are tested at 100 K and the I–V curves are shown in Fig. 3(a). It can be seen clearly that the operating voltage of the sample after aging is higher than before aging at the same current. The increase of voltage at high current indicates the increase of resistance after aging. Thus, the series resistances for samples are calculated by I–V curves according to Ref. [19]. The slope of $(I\mathrm{d}V/\mathrm{d}I)$ *versus* I is identified to calculate the series resistance of LED. As shown in Fig. 3(b), the series resistance increases from 8.46 Ω to 10.20 Ω at 100 K. The increase of the series resistance may be due to the reversible dissociation of Mg–H complexes on the p-type side of the device, which is attributed to the self-heating effect during aging.[20] The Mg–H complexes are dissociated in the initial stage of the aging, then the dissociated H reacts with Mg_{Ga}, thus forming new Mg–H complexes or metastable Mg–H_2 complexes. Thereby the effective doping of the p-type layer decreases, which is responsible for the increase of series resistance. These complexes can also act as impurity levels respectively at about 0.12 eV and 0.22 eV above the valence band edge. Additionally, these impurity levels can consume partial carriers.[21]

The EL spectra tested at 100 K are plotted on a logarithmic scale as shown in Figs. 4(a) and 4(b). The sample before and after aging has three peaks which are marked as P_1, P_2, and P_3. The cross sectional TEM image of the V-pits of analyzed sample is shown in Fig. 4(c), which displays the V-pit tip originating from SLs and embedded in MQWs. Additionally, the EBL and MQWs on c-plane are 3–5 times thicker than those on sidewall of V-pits. Also, in view of the existence of the V-pits in LED epitaxial structure, the transport path of holes via V-pits will change after aging. As shown in Fig. 4(d), there are five directions for holes' injection: (I_1) injection into c-plane QWs through the flat c-plane region, (I_2) injection into c-plane QWs via the sidewall of V-pits, (I_3) injection into QWs of sidewall of V-pits and partaking in radiative recombination, (I_4) non-radiatively recombination at dislocations in V-pits, (I_5) injection through the sidewall of the V-pits and recombination in SLs radiatively.[22,23] According to the transport path of holes, P_1 is the main emission peak of the c-plane MQW, whose wavelength is around 550 nm at typical 35 A/cm^2 and shows a blue-shift with current density increasing. As for the short-wavelength emission, it can be seen clearly that P_2 appears at about 500 nm (35 A/cm^2) and P_3 with a shorter wavelength for about 445 nm (35 A/cm^2). P_2 is different from P_1 and P_3, and is considered as the broadened emission of the sidewall MQWs in the V-pits.[17,20] In addition, P_3 is attributed to the emission from the InGaN/GaN SLs sandwiched between the n-type GaN and MQW active layer.[18] So, as can be seen in EL spectra, the emission of P_2 is attributed to the I_3 direction of holes injection. P_3 comes from SLs. Due to the thickness of the top MQWs and multi quantum barriers (MQBs), it is hard for holes to be injected along the c-axis direction, while they can be more easily injected through the sidewall of V-pits along the direction I_5 bypassing the top yellow MQWs.

It is noteworthy that although the sample has three peaks both before and after aging, the EL intensities of P_2 and P_3 for the sample after aging are much higher than those before aging, especially for P_3. This indicates that the number of holes injected into SLs for sample after aging is more than before ag-

ing, namely after aging, less holes are injected into the MQWs. Additionally, after aging, P_2 and P_3 start to appear earlier with the increase of current density. It can be seen in Fig. 4(b) that after aging the P_2 and P_3 start to appear when the current density is 0.18 A/cm^2, while before aging they start to appear at 0.75 A/cm^2 as indicated in Fig. 4(a). The phenomenon indicates that after aging the holes are more easily transferred into the SLs.

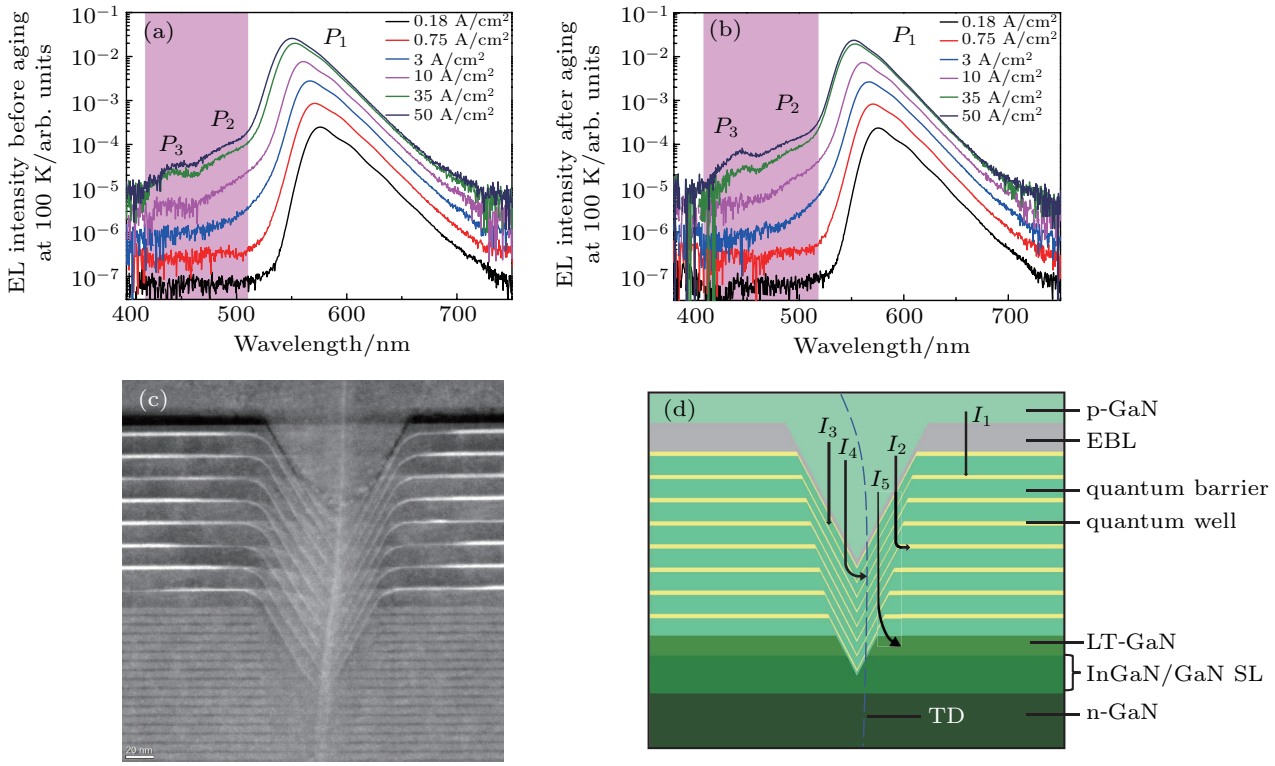


Fig. 4. EL spectra of samples before (a) and after (b) aging as a function of injection current at 100 K. (c) Cross sectional TEM image of the V-pits. (d) Image showing different ways of injecting holes via V-pits.

Because the EBL in the *c*-plane region is 3–5 times thicker than on the sidewall of V-pits. The quantity of Mg–H complex in the *c*-plane region is more than on the sidewall of V-pits. After aging, the resistance increases more in the *c*-plane region than on the sidewall of V-pits, and the voltages applied to these two regions also show a similar change. This increase in voltage can compensate for the energy barrier provided by the sidewall of V-pits, making more holes' current flow via the sidewall of V-pits and injected into the SLs than before aging.[24] In other words, the more holes are injected into the SLs, the less holes are injected into the QWs, which can reduce the current participated in radiative recombination in MQWs at 100 K, further lead LOP to decrease. Note that here, the holes' injection mechanism for the sample after aging is changed at cryogenic temperature, and this mechanism may change for devices at room temperature, even reduce the LOP, which needs further investigating in the future.

4. Conclusions

In this paper, the aging mechanism of yellow GaN-based LEDs with V-pits on Si substrates is investigated. It is found experimentally that the decay of LOP is mainly attributed to the increase of SRH recombination. Furthermore, the aging process causes the degradation in the p-side layer, and induces the voltage applied to the *c*-plane region and the side wall of V-pits to change. Based on the EL spectrum at 100 K, this voltage change causes more holes to be injected into SLs via sidewall of V-pits, which means that less current participates in radiation recombination in MQWs after aging than before aging. This mechanism may also work for devices at room temperature, which needs further investigation in the future.

References

[1] Tsao J Y, Crawford M H, Coltrin M E, Fischer A J, Koleske D D, Subramania G S and Jr R F 2014 *Adv. Opt. Mater.* **2** 809
[2] Zhang J, Xiong C, Liu J, Quan Z, Wang L and Jiang F 2014 *Appl. Phys. A* **114** 1049
[3] Tao X, Liu J, Zhang J, Mo C, Xu L, Ding J and Pan S 2018 *Opt. Mater. Express* **8** 1221
[4] La Grassa M, Meneghini M, De Santi C, Mandurrino M, Goano M, Bertazzi F and Zanoni E 2015 *Microelectron. Reliab.* **55** 1775
[5] Buffolo M, De Santi C, Meneghini M, Rigon D, Meneghesso G and Zanoni E 2015 *Microelectron. Reliab.* **55** 1754
[6] Zhang N, Wei X C, Lu K Y et al 2016 *Chin. Phys. Lett.* **33** 117302
[7] Barton D L, Osinski M, Perlin P, Eliseev P G and Lee J 1999 *Microelectron. Reliab.* **39** 1219
[8] Meneghini M, Podda S, Morelli A, Pintus R, Trevisanello L, Meneghesso G and Zanoni E 2006 *Microelectron. Reliab.* **46** 1720

[9] Fu J, Zhao L, Cao H, Sun X, Sun B, Wang J and Li J 2016 *AIP Adv.* **6** 055219
[10] Hsu C Y, Lan W H and Wu Y S 2003 *Appl. Phys. Lett.* **83** 2447
[11] Kim J, Cho Y H, Ko D S, Li X S, Won J Y, Lee E and Kim S 2014 *Opt. Express* **22** A857
[12] Han S H, Lee D Y, Shim H W et al 2013 *Appl. Phys. Lett.* **102** 251123
[13] Li C K, Wu C K, Hsu C C, Lu L S, Li H, Lu T C and Wu Y R 2016 *AIP Adv.* **6** 055208
[14] Li Y, Yun F, Su X, Liu S, Ding W and Hou X 2014 *J. Appl. Phys.* **116** 123101
[15] Kim K S, Han D P, Kim H S and Shim J I 2014 *Appl. Phys. Lett.* **104** 091110
[16] Han D P, Zheng D G, Oh C H, Kim H, Shim J I, Shin D S and Kim K S 2014 *Appl. Phys. Lett.* **104** 151108
[17] Zhu D, Xu J, Noemaun A N, Kim J K, Schubert E F, Crawford M H and Koleske D D 2009 *Appl. Phys. Lett.* **94** 081113
[18] Han D P, Oh C H, Zheng D G, Kim H, Shim J I, Kim K S and Shin D S 2015 *Jpn. J. Appl. Phys.* **54** 02BA01
[19] Schubert E F 2006 *Light–emitting diodes* (Cambridge, New York, Melbourne, Madrid, Cape Town, Singapore, São Paulo: Cambridge University Press)
[20] Pavesi M, Manfredi M, Salviati G, *et al*. 2004 *Appl. Phys. Lett.* **84** 3403
[21] Salviati G, Rossi F, Armani N, *et al*. 2004 *Eur. Phys. J.-Appl. Phys.* **27** 345
[22] Tao X X, Mo C L, Liu J L, *et al*. 2018 *Chin. Phys. Lett.* **35** 057303
[23] Quan Z, Wang L, Zheng C, Liu J and Jiang F 2014 *J. Appl. Phys.* **116** 183107
[24] Wu X, Liu J and Jiang F 2015 *J. Appl. Phys.* **118** 164504